

University of Tartu
Faculty of Mathematics and Computer Science
Institute of Computer Science

Ilja Kuzovkin

Pattern recognition for non-invasive EEG-based BCI

Bachelor's thesis

Supervisor: Konstantin Tretyakov

Author: "....." june 2011

Supervisor: "....." june 2011

Approved for defence

Professor: "....." june 2011

Tartu 2011

Contents

Introduction	5
1 Biological Background and Electroencephalogram	7
1.1 Nature of the signal	7
1.2 Electroencephalogram	8
1.2.1 EEG technology	9
1.2.2 Electrode placement	9
1.2.3 Frequency ranges	11
1.2.4 Devices we used during the work	12
2 Signal Processing	15
2.1 Discrete Fourier Transform	15
2.2 Input signal	16
2.3 Data representation as instances and attributes	17
2.4 Instance classes	17
3 Machine Learning Algorithms	19
3.1 OneR	19
3.2 J4.8	20
3.3 Naïve-Bayes	20
3.4 Support Vector Machines	21
4 Applying Machine Learning Techniques	22
4.1 Eye blinks	23
4.2 Left and Right	24
4.3 Affective pictures	24
4.4 Results	31
Summary	33
Acknowledgements	34
Resümee	35

Introduction

Research on BCI (Brain-Computer Interface) devices began in the 1970s [wika]. Mainly research and development have been focused on restoring human abilities such as sight, hearing and motor functions.

One of the most exciting areas of BCI research is the development of devices that can be controlled by thought. Some of the applications of this technology may seem unserious, such as the ability to control a video game by thought. However, there is more significant purpose – devices that would allow severely disabled people to function independently. For a quadriplegic, something as basic as controlling a computer cursor via mental commands would represent a revolutionary improvement in the quality of life.

There are many techniques, which can allow to read brain's activity. Two main subgroups are *invasive* and *non-invasive* devices [wika]. Invasive devices provide much better signal, high signal-to-noise ratio and wide frequency range, but they must be surgically implanted into the subject's brain. Non-invasive devices are easy to deploy, they are cheaper, but their signal quality is much worse, high level of noise is produced by skull and skin. This is the reason why signal processing becomes very important – we want to gather as much useful information from this noisy data as possible.

During the past 5 years several companies [con] came up with devices aimed at a wide range of users. These products are positioned as the new generation of human interface devices (HID¹) that will allow people to manipulate their personal computers and play video games using thought. However, current EEG-based non-invasive BCIs can not yet provide such level of control. Even the most recent and advanced of these devices, the Emotiv EPOC [emo] allows to recognize only four mental states to manipulate objects on the screen. It is obvious that four actions is not enough for playing a game. Moreover, handling four different mental states is difficult for the user and requires special training. To somehow fix that, companies supply their devices with additional sensors and try to combine signals from brainwaves, muscle activity and other inputs to reach better result. Our work is focused on the question of how much it is possible to achieve by reading brainwaves only.

¹Type of computer device that interacts directly with user and takes input from him.

During the work we used data from two non-invasive EEG devices. The first one is the Emotiv EPOC we mentioned before. The second one is a more sophisticated Biosemi ActiveTwo DC amplifier with 32 electrodes. We ran several experiments on the datasets trying to distinguish event occurrences using machine learning classification algorithms.

The work is divided into five chapters. Chapter 1 gives a biological background, the basic introduction to EEG technology and the description of devices we use. Chapter 2 describes the steps we performed to process the raw signal data and prepare it for use in the classification algorithms. Chapter 3 briefly describes the classification algorithms we use. In the chapter 4 we present the results of our experiments and give the conclusion.

Chapter 1

Biological Background and Electroencephalogram

1.1 Nature of the signal

First let us see what allows us to monitor brain activity and what exactly this activity represents. There are special cells, called neurons, in our brain. These are an electrically excitable cells that process and transmit information via electrical and chemical signaling [wikb]. The signals we try to capture are generated by changes in the electrical charge of the membrane of the neuron. Neurons have a *resting potential*, which is the difference in the electrical potential between

the interior of a cell and extracellular space. The resting potential fluctuates as a result of impulses arriving from other neurons through synapses. Cell membrane contains ion channels where ions, such as sodium, potassium, chloride and calcium are concentrated during the chemical processes in the cell. This generates cross-membrane voltage differences. Changes in the cross-membrane voltage generate *postsynaptic potentials* which cause electrical flow along the membrane and dendrites [Fis91].

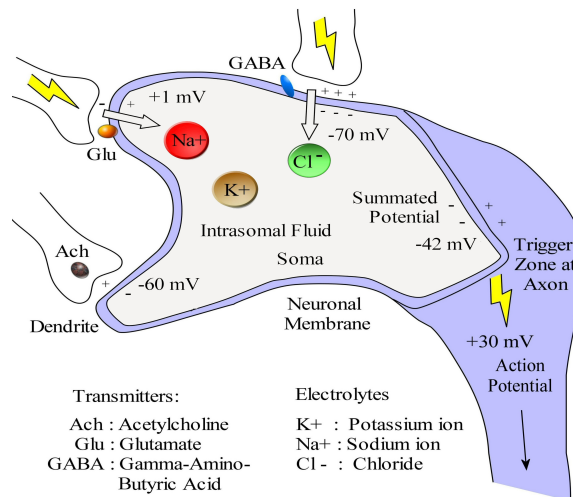


Figure 1.1: Summation of postsynaptic potentials. [Won10]

When a summated potential at the trigger zone of the axon reaches the threshold of -43 mV for instance, it fires the axon by generating an *action potential* of $+30$ mV that goes along the axon to release the transmitters at the end of the axon (see Figure 1.1). When a summated potential is below the threshold, the axon rests. This summation can be observed well at the vertically oriented pyramidal cells of the cerebral cortex due to following properties of these cells:

- The dendrites of the pyramidal cells extend through nearly all layers of the cortex, guiding the flow of currents generated by postsynaptic potentials from the deep layers to the more superficial ones.
- These cells are closely packed and oriented parallel to each other, facilitating spatial summation of the currents generated by each neuron.
- Groups of these neurons receive similar input and respond to it with potentials of similar direction and timing.

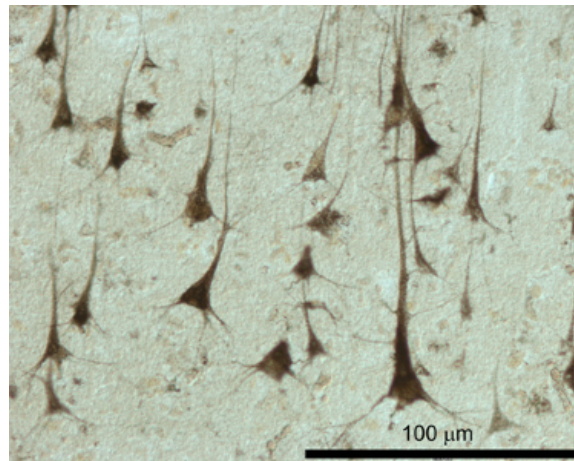


Figure 1.2: Pyramidal cells in layer five of the human auditory cortex. [waud]

Despite the fact that most of the currents remain inside the cortex, small fraction penetrates to the scalp, where it causes different parts of the scalp to have different electric potentials. These differences, having amplitudes of usually $10-100$ μV are detected by electrodes and constitute the electroencephalogram (EEG).

1.2 Electroencephalogram

By observing differences between electrical signals coming from the different locations on the scalp, we can monitor brain activity and see which parts

of the brain are active during different types of activities and how high the activity is.

1.2.1 EEG technology

EEG mainly reads *postsynaptic potentials*, which are relatively sustained (a potential persists up to 100 msec). The *active potentials* (actual neuron firings) are very brief (1 msec) and their electrical contribution is small, so we cannot track them on the EEG. If we could be able to see these exact moments when neuron sends the signal, it could give us much more information.

As we mentioned before, electrodes read potentials and show differences between them. Usually there is one or several *reference electrodes* which are placed on the most electrically stable areas, such as nose or ears. Other electrodes' potentials are being compared with reference ones.

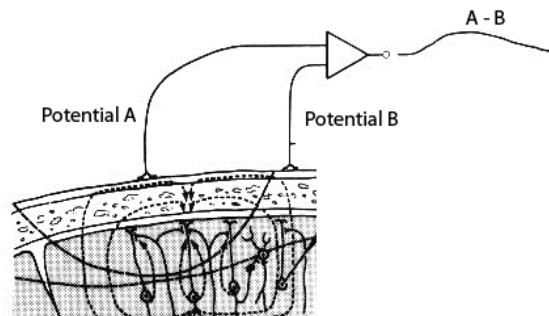


Figure 1.3: Two electrodes on scalp areas with different electric potentials produce the signal. [Fis91]

1.2.2 Electrode placement

The question of placing the electrodes is important, because different lobes of cerebral cortex are responsible for processing different types of activity (see Table 1.1).

Letter	Lobe	Functions
F	Frontal lobe	<ul style="list-style-type: none"> • recognize future consequences resulting from current actions • choose between good and bad actions (or better and best) • determine similarities and differences between things or events
T	Temporal lobe	<ul style="list-style-type: none"> • auditory perception • processing of semantics of speech and vision • long term memory

Letter	Lobe	Functions
C	Central lobe (actually: Motor cortex and Somatosensory cortex)	<ul style="list-style-type: none"> • planning, control, and execution of voluntary motor functions • sense of touch
P	Parietal lobe	<ul style="list-style-type: none"> • spatial sense and navigation • sensory information from various parts of the body • knowledge of numbers and their relations • manipulation of objects
O	Occipital lobe	<ul style="list-style-type: none"> • visual processing center

Table 1.1: Lobes and their functions

The most common placement system is called the “10-20 system”. Each electrode name consists of two parts – the letters and the numbers. The letters correspond to the first letter of the name of the lobe. Numbers just enumerate electrodes on the same lobe, where left channels are numbered with odd numbers, right channels with even numbers (see Figure 1.4).

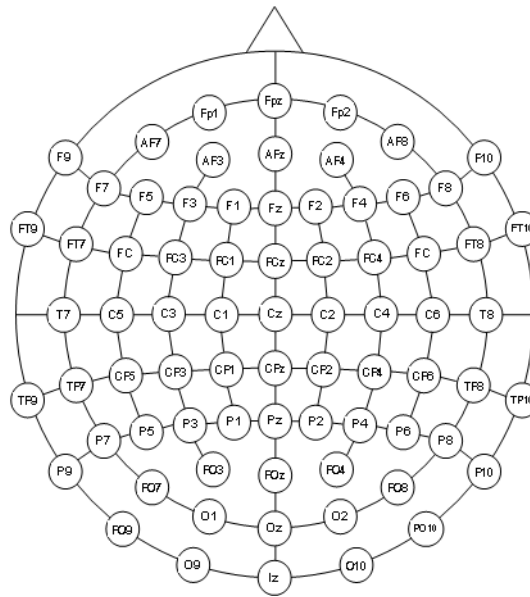
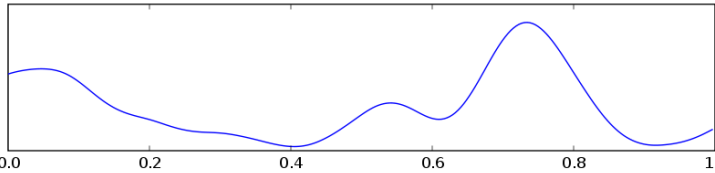
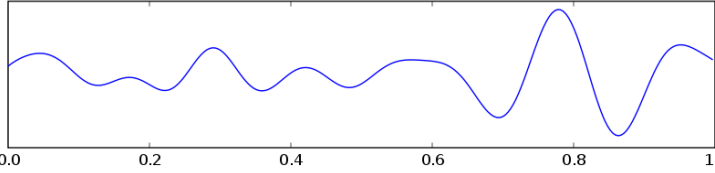
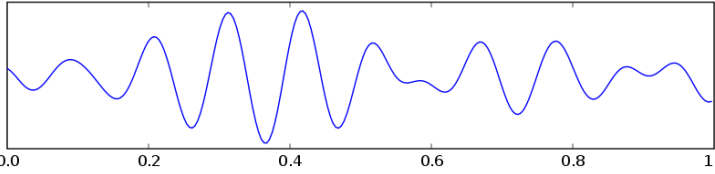


Figure 1.4: Placement of 64 channels in 10-20 system.

1.2.3 Frequency ranges

The EEG signal can be decomposed into several components according to frequency. These components are divided into categories and are believed to represent different types of brain activities (see Table 1.2). For example a particular periodic component with frequency 13 to 40 Hz is called *Beta rhythm* and appears in the signal during active, anxious thinking and concentration.

Name	Type of activity
<i>Delta</i> up to 4 Hz	<ul style="list-style-type: none"> • adults slow wave sleep • babies brain activity • Continuous attention tasks [KABG⁺06] 
<i>Theta</i> 4–8 Hz	<ul style="list-style-type: none"> • young children brain activity • drowsiness or arousal • idling • Person is actively trying to repress a response or action [KABG⁺06] 
<i>Alpha</i> 8–13 Hz	<ul style="list-style-type: none"> • wakeful relaxation • eyes are closed • inhibition of areas of the cortex not in use, plays an active role in network coordination and communication. [PP07] 

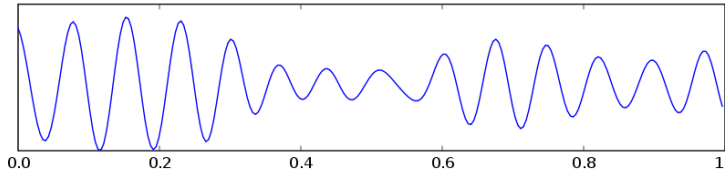
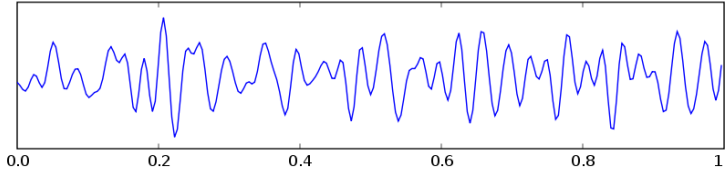
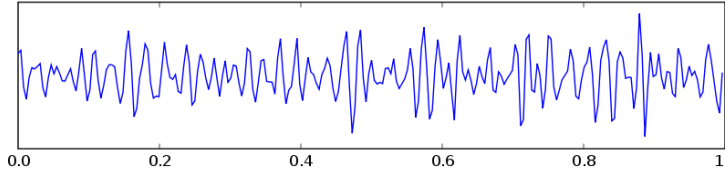
Name	Type of activity
<i>Mu</i> 8–13 Hz	<ul style="list-style-type: none"> • Appears in resting neurons responsible for motor activity 
<i>Beta</i> 13–30 Hz	<ul style="list-style-type: none"> • alert • active, anxious thinking, concentration • work 
<i>Gamma</i> 30–100+ Hz	<ul style="list-style-type: none"> • Cross-modal sensory processing (perception that combines two different senses, such as sound and sight) [KC06] [KSO07] [NYC04] • Appears during short term memory matching of recognized objects, sounds, or tactile sensations [HFL10] 

Table 1.2: Basic frequency ranges and corresponding activity types

1.2.4 Devices we used during the work

In our experiments we used data from two EEG devices. Here we will give a brief overview of their specifications and features.

Emotiv EPOC

Emotiv EPOC was released in December 2009 by Emotiv Systems as a device for a wide audience, which allows to train the model for recognizing certain mental states, use this model afterwards for detecting user’s current mental state and perform an action mapped to this state. Ideally, this should allow the user to play video games using power of thought. Along with brain activity, data about muscle activity is also being detected by the device as it interferes with the EEG signal. Consequently it is also possible to map a custom action to the blinking of an eye, moving the eyes to the left or to

the right, smiling and several other mimical actions.

Emotiv EPOC is available to the wide range public due to its pricing. The most low-priced edition (*Limited edition*) costs \$299. However, this edition, as well as the \$500 *Developer edition* have a severe limitation – it is not possible to obtain the raw data from the device. Signal is encrypted with an AES key, which makes this device incompatible with third-party software and drivers as OpenViBE [YR10]. To be able to read raw data the user has to obtain the *Research edition*, which costs \$750 [emo]. Except for the encryption key the device itself is the same in all editions. The difference between them lies in the software. Only *Research editions* has software to read raw signal, process it and export, and libraries, which allow using the API¹ in third-party applications.

Emotiv EPOC has 14 wet electrodes which correspond to the following electrodes in 10-20 system.

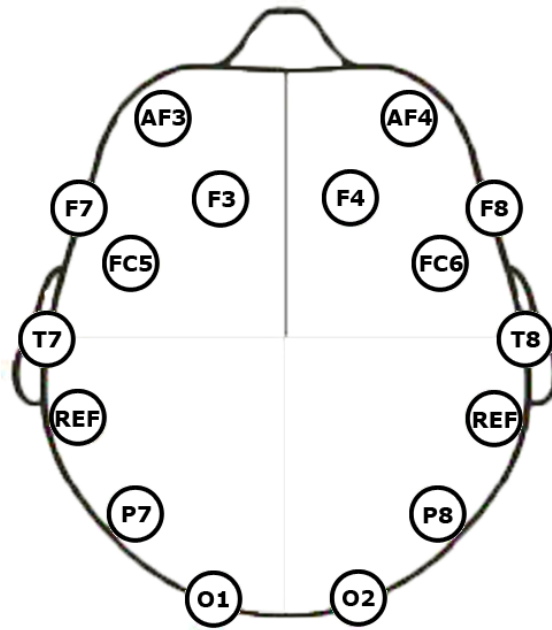


Figure 1.5: Emotiv EPOC: 14 electrodes and 2 reference channels

Biosemi ActiveTwo

This is high-end a device used in many universities for research [biob]. Our data was recorded on a 32-electrode version. This device has all the neces-

¹Application Programming Interface is a particular set of rules and specifications that software programs can follow to communicate with each other.

sary software with it. Cost of the suit is significantly higher – around 20000 euros [bioa].

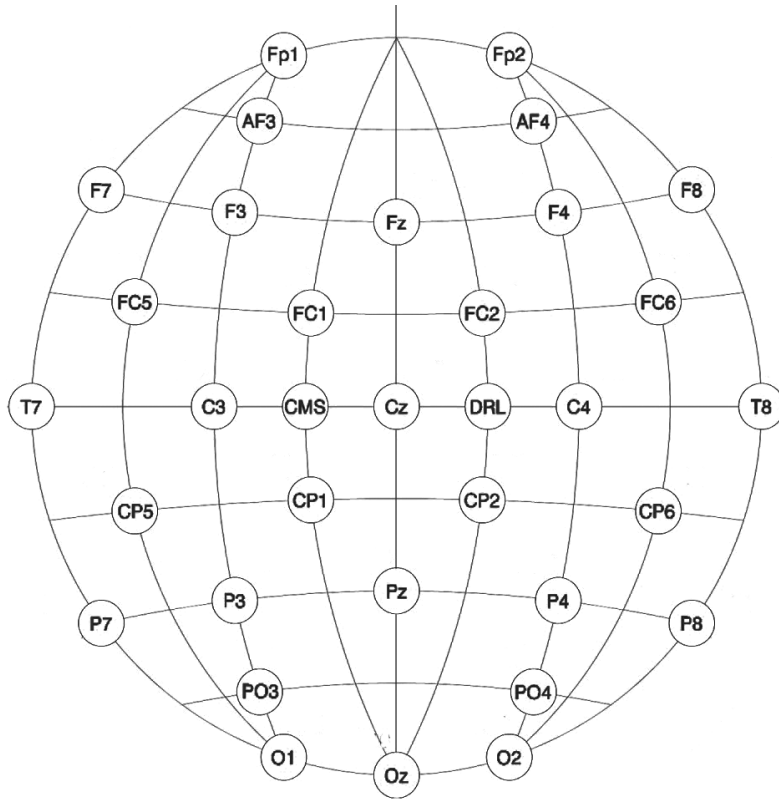


Figure 1.6: Biosemi ActiveTwo with 32 electrodes and 2 reference channels

Chapter 2

Signal Processing

Our primary goal is to find patterns and some kind of structure in the raw signal we get from the EEG device. So we have to come up with an idea how to process the raw signal and represent it in a form classification algorithm could deal with. The most common type of data representation is a set of *instances* where each instance is a fixed-length vector of real values. Instance has *attributes* which characterize it, and each instance belong to the certain class.

2.1 Discrete Fourier Transform

We split the signal into *windows* of length l seconds. On each window we use Discrete Fourier Transform (DFT) to decompose the signal into its frequency components and use each frequency component as an attribute. The DFT representation of a signal is given by the formula

$$v_i = \sum_{n=0}^{N-1} x_n e^{-\frac{2\pi i}{N} kn}$$

where N is the number of values of a signal measured during the the period of time (the window), x_n ($n \in \{0 \dots N - 1\}$) is the value of the signal measured in the time point n , v_n ($n \in \{0 \dots N - 1\}$) is a complex amplitude of sinusoidal signal, which together sum up to the initial signal. The magnitude of x_n corresponds to the contribution of a complex exponential component into initial function.

On the Figure 2.1 frame A denotes the window we take. Red bars on the right are magnitudes of sinusoidal functions. For example second red bar shows how big is contribution of sinusoidal functions with frequency 2 to 4 Hz into the signal inside the A frame on the left. Each of these bars will be considered later as an attribute of an instance. In this example l is 0.3 seconds, sampling rate 128 Hz, so the resulting size of the window is $128 \cdot l = 38$ instances per window.

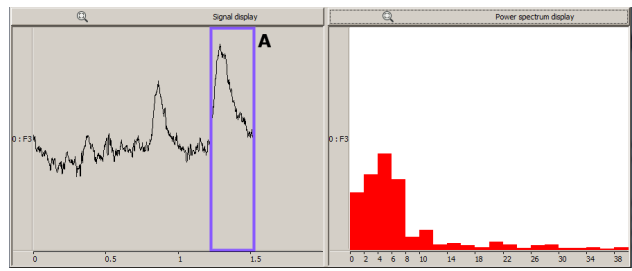


Figure 2.1: Window of the length of 0.3 seconds with a spike (eye blink) and result of DFT performed on it.

2.2 Input signal

The signal we receive from our EEG devices consists of 14 (Emotiv EPOC) or 32 (Biosemi ActiveTwo) separate signals – one signal per electrode (see Figure 2.2). These two devices use different sampling rate for analog signal discretization: 128 Hz with Emotiv EPOC and 256 Hz with Biosemi ActiveTwo.

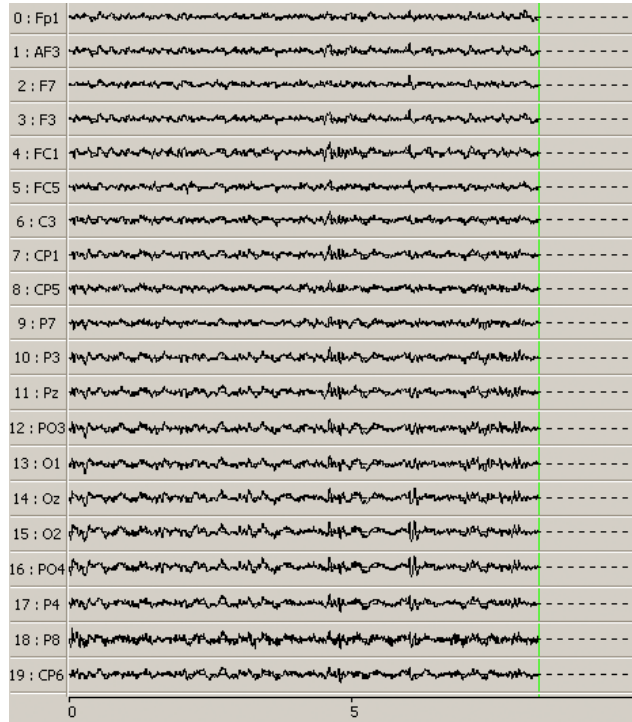


Figure 2.2: Signals from multiple channels

2.3 Data representation as instances and attributes

We treat each signal in the way described in the Section 2.1 – split it into the windows as compute DFT of each window (see Figure 2.3).

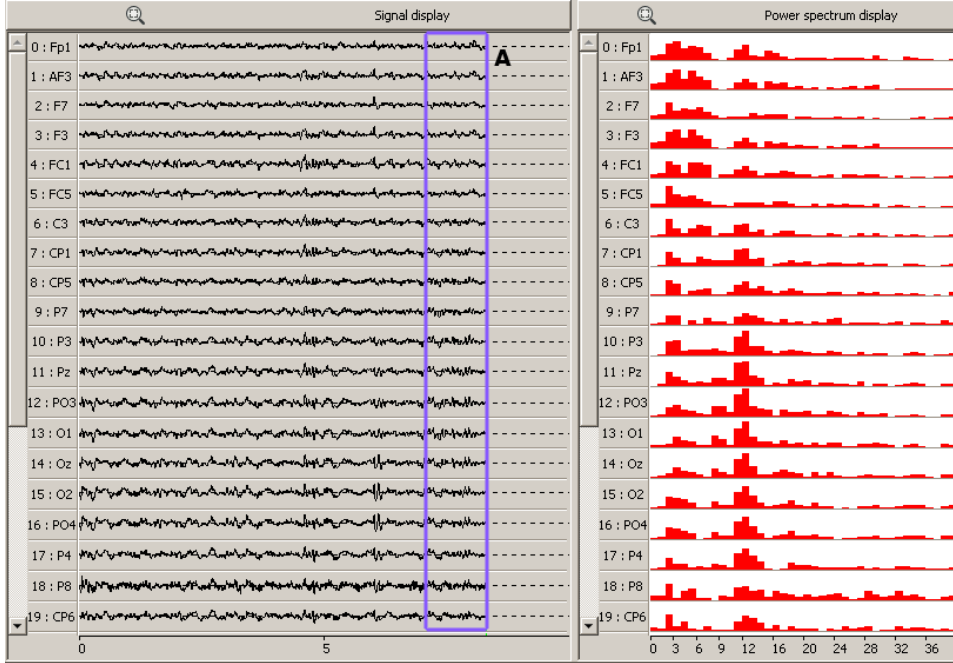


Figure 2.3: DFT of the window on several channels

For each window we join the the spectra of all channels into a single vector of length $m = c \cdot n$, where c in number of electrodes and n is number of components in the DFT. Each red bar represent an attribute: for example attribute with name `AF3_2Hz` is power of frequency 2Hz at channel AF3, `O7_4Hz` is power of frequency 4Hz at channel O7, also we can group several frequencies into one attribute like `AF3_8-12Hz`.

Table 2.1 present an example of the resulting dataset. Rows represent instances (windows), from the timing in the first column we can see $\tau = 0.1$ second, number of electrodes (channels) is 32 and for each channel we have 40 attributes – one per 1 Hz. Last column specifies class of the instance. This dataset was recorded while showing affective pictures to the subject: `pos` means positive picture and `bld` – picture with blood on it.

2.4 Instance classes

During the experiments at certain points of time the subject is asked to perform an action. For example to blink an eye. Or to have a look at a picture. We mark these moments of time, so later we know where exactly

Time	Channel 1 spectrum					...	Channel 32 spectrum				Class
	ch1hz1	ch1hz2	...	ch1hz40	...	ch32hz1	ch32hz2	...	ch32hz40		
0.1	1.92	2.90	...	54.53	...	15.65	21.43	...	73.40	pos	
0.2	100.54	71.53	...	10.44	...	4.30	10.46	...	37.08	pos	
0.3	61.64	86.96	...	17.35	...	8.54	7.76	...	50.26	pos	
...	
1.5	58.48	5.23	...	99.94	...	11.21	12.96	...	44.29	pos	
1.6	95.51	87.85	...	115.73	...	112.04	159.52	...	78.44	bld	
1.7	45.43	67.82	...	90.19	...	33.20	118.63	...	94.47	bld	
1.8	20.71	35.52	...	94.69	...	24.21	34.12	...	51.83	bld	
...	
3.0	59.90	12.02	...	141.65	...	10.33	16.23	...	78.16	bld	

Table 2.1: Example of a dataset

to look for a brain reaction. After we decompose the signal, we assign certain class to each instance. For example in the Table 2.1 the subject was observing a positive picture for the first 1.5 seconds, so after we split the signal into instances we assign `pos` class to each window, which includes these moments of time.

Chapter 3

Machine Learning Algorithms

Machine learning is a common name for various techniques, which have the same purpose – look for patterns and structure in the data. The general task of classification algorithm is finding the *classifier* from a set of classified instances (x, y) where x is a vector of attributes and y is the class. Classifier is a function $y = f(x)$ which maps instance with a class. During our work we use WEKA [PR04] software and the algorithms implemented in it. In this chapter we briefly describe the four algorithms we applied on our data.

3.1 OneR

This algorithm is simple and cheap in the sense of computational resources. Set of rules is created for each attribute, then algorithm checks error rate of this set of rules and finally selects the set where error rate is the smallest one. OneR can be described in pseudocode as follows [WF05]

```
For each attribute
  For each value of this attribute
    count how often each class appears
    find most frequent class
    add a rule to assign this class to this attribute-value
  Calculate error rate for resulting set of rules
Choose set of rules with smallest error rate
```

In other words algorithm finds the attribute, which best predicts the class relying only on this single attribute to make decisions. It is quite naive, but frequently achieves high accuracy levels. Perhaps this is because most of the data is highly redundant and often one attribute is sufficient to determine the class of the instance.

3.2 J4.8

J4.8 is the WEKA implementation of the C4.5 algorithm, which is a very popular decision tree learning algorithm [WF05]. The general idea of a decision tree learning algorithm is the following:

1. Choose one attribute from the set and place it as the root node of the tree.
2. Make one branch for each possible value of the attribute (or for group of values).
3. Repeat step 2 recursively for each branch
4. If all instances in a subset have the same class, stop recursion into this branch and go to the next one

The main difference between different decision tree learning algorithms is in the way how step 1 is implemented. Additionally each algorithm can have specific parameters. J4.8 has two main parameters: *confidence value*, used for pruning and minimum number of instances per leaf (for more details see textbook [WF05]).

3.3 Naïve-Bayes

This algorithm is an example of a statistical modeling technique. We assume that all attributes are independent of one another. This is where *Naïve* part comes from. In real life, attributes are in most cases not independent. But this assumption gives us a simple model that often performs surprisingly well [WF05].

The method is based on the Bayes formula of conditional probability

$$\Pr[A|B] = \frac{\Pr[B|A] \cdot \Pr[A]}{\Pr[B]}$$

Let E be vector of attributes (x_1, x_2, \dots, x_n) and C be the class of an instance, then, applying the formula we get

$$\Pr[C|E] = \frac{\Pr[E|C] \cdot \Pr[C]}{\Pr[E]} \propto \Pr[E|C] \cdot \Pr[C]$$

(we can drop the denominator, because we can normalize the probabilities of all attributes to sum to 1). If we assume conditional independence of the attributes, then

$$\Pr[E|C] \cdot \Pr[C] = \Pr[x_1|C] \cdot \Pr[x_2|C] \cdot \dots \cdot \Pr[x_n|C] \cdot \Pr[C]$$

where $\Pr[x_i|C]$ can be estimated from the training data.

Assumption of independence is needed because only independent probabilities can be multiplied together. One thing can go wrong with pure Bayes approach – if any particular attribute does not occur in training set in conjunction with every class. In this case multiplication will give 0 and the whole probability will be 0 as well. In Naïve-Bayes classification algorithm this problem is avoided by adding small ϵ to the values.

3.4 Support Vector Machines

Support Vector Machines (SVM) is linear model algorithm. The idea of the algorithm is to find linear separation boundary between the class instances, which correctly separates the instances into the classes. This boundary must have *maximal margin* – distance to the closest training sample instances is the maximal one (see Figure 3.1).

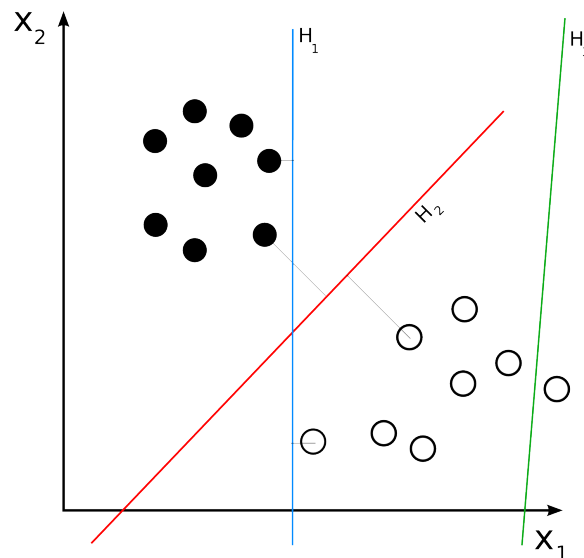


Figure 3.1: H_3 doesn't separate the two classes. H_1 does, but with a small margin and H_2 separates the instances with the maximum margin. [wikc]

Support vector machines can also work in non-linear space. This is achieved by transforming instances space into a new space and use non-linear mapping between them. With a nonlinear mapping straight line in the new space doesn't look straight in the original space. In such way linear model constructed in the new space can represent a nonlinear decision boundaries in the original space [WF05].

We use WEKA implementation of SVM, which is called SMO. In our experiments we use only linear kernel in the algorithm.

Chapter 4

Applying Machine Learning Techniques

In this chapter we apply previously described algorithms on three different datasets.

The first data set (Eye blinks) is recorded using Biosemi ActiveTwo device. Subject was asked to blink both eyes every 5 seconds during one minute.

Second one (Left and right) is recorded using Emotiv EPOC. Subject was alternating *left* and *right* mental states every 20 seconds during 4 minutes.

The last and most interesting dataset (Affective pictures) was kindly provided by colleagues from department of experimental psychology. 360 pictures were shown to the subject. Pictures were ranked into 5 types: sexual, positive, neutral, negative and bloody. Picture was displayed on the screen for 1.5 seconds. Our task was to train the model which could distinguish which kind of picture is being shown to the subject at the moment.

During the experiments we measure three characteristics: *accuracy*, *precision* and *recall*. To define them we use such terms as *true positives*, *true negatives*, *false positives* and *false negatives*. In the context of classification tasks true positives represents the amount of the instances, which belong to the class *A* and were classified accordingly. True negatives show number of instances which do not belong to the class *A* and were classified accordingly. False positives represent amount of instances classified as class *A*, but really they belong to some other class *B*. And false negatives show the number of instances classified as class *B*, however they belong to the class *A*.

Using these terms we define accuracy as

$$A = \frac{\text{true positives} + \text{true negatives}}{\text{true positives} + \text{true negatives} + \text{false positives} + \text{false negatives}}$$

In other words accuracy shows amount off all instances classified correctly.

We define precision as

$$P = \frac{\text{true positives}}{\text{true positives} + \text{false positives}}$$

which shows for each class percentage of correct instances among those that the algorithm believes to belong to the class. And we define recall as

$$R = \frac{\text{true positives}}{\text{true positives} + \text{false negatives}}$$

percentage of correct instances among all instances that actually belong to the relevant class. To describe result of the algorithm with one number we use *F1 score* defined as

$$F1 = 2 \cdot \frac{\text{Precision} \cdot \text{Recall}}{\text{Precision} + \text{Recall}}$$

When we have several classes in the dataset the weighted average values are used in this formula. Everywhere later in the text if we say "result is $n\%$ " we mean F1 score.

4.1 Eye blinks

The first test we performed was classification of the signal where test subject blinks both eyes every 5 seconds. Because of muscle activity, eye blinks strongly affect EEG and are perfectly visible even on the visualized raw signal (see Figure 4.1).

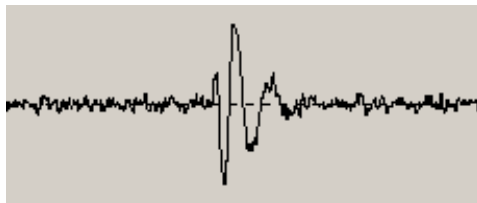


Figure 4.1: Eye blink on the raw signal

Our goal here is to check how well our approach and methodology work. We take 60 seconds of data, split it into two parts (6 blinks in each). Model trained on the first part (524 instances with a blink and 3534 instances without a blink) applied to the second part (459 instances with a blink and 3471 without) gave the following the results:

Algorithm	Accuracy	Precision	Recall
OneR	94.4%	72.2%	83.9%
J48	94.0%	69.2%	87.6%
Naïve-Bayes	93.6%	65.3%	96.9%
SMO	95.9%	76.7%	93.2%

Table 4.1: Recognition of the eye blinks

In the Table 4.1 we see that eye blinks can be detected reasonably well. F1 score with the SMO algorithm is 84.15%. Next we try something more complicated and closer to our research.

4.2 Left and Right

The next dataset we are going to work with was recorded on a subject who was trying to move a box on a computer screen with mind only. No mimics or any other motor activity was engaged. We will refer mental actions the subject engaged as *mental states*. The training set consists of 60 seconds of *left* mental state (565 instances) and 60 seconds of *right* mental state (629 instances). And the test set of 20 seconds of *left* (245 instances) and 20 seconds of *right* (597 instances).

Algorithm	Accuracy	Class	Precision	Recall
OneR	67.2%	left	43.7%	76.9%
		right	42.5%	77.2%
J48	76.4%	left	57.6%	86.9%
		right	71.0%	78.6%
Naïve-Bayes	84.1%	left	73.6%	88.1%
		right	65.0%	89.6%
SMO	80.3%	left	65.1%	87.2%
		right	69.8%	84.6%

Table 4.2: Distinguishing between left and right mental states

F1 score is 84.0% with Naïve-Bayes algorithm. This is pretty good result especially considering how small our training set was.

4.3 Affective pictures

This dataset consists of 360 *epochs* of length 1.5 seconds each. One epoch shows the brain activity while subject was observing the affective picture. We run a number of experiments on this dataset varying input data parameters. We train the model on the first 66% of the data (238 pictures) and test it on the rest 33% (122 pictures).

In the process of converting frequency power bands to the instances for classification algorithms we can adjust two parameters:

- Size of the window l
- Sampling frequency $\omega = \frac{1}{T}$ – how many windows per second we take

In this section we are going to see how adjusting these parameters will affect final result. During the first two attempts we do not use moving window, but compute DFT just once for the particular part of the epoch to get frequency characteristic of that part.

DFT of the whole epoch ($l = 1.5, \omega = 1$)

Here we compute band powers of the whole epoch of 1.5 seconds – all of the time subject was observing the picture. Number of instances in the dataset is 72 per each type of the affective picture.

Algorithm	Accuracy	Class	Precision	Recall
OneR	29.5%	sex	32.4%	39.3%
		pos	33.3%	28.0%
		ntr	28.6%	26.1%
		neg	25.0%	23.8%
		bld	26.9%	28.0%
J48	17.2%	sex	18.2%	14.3%
		pos	15.2%	20.0%
		ntr	18.2%	8.7%
		neg	12.5%	9.5%
		bld	20.0%	32.0%
Naïve-Bayes	13.1%	sex	23.1%	10.7%
		pos	17.6%	12.0%
		ntr	0%	0%
		neg	9.3%	19.0%
		bld	17.1%	24.0%
SMO	16.4%	sex	17.6%	10.7%
		pos	25.9%	28.0%
		ntr	12.9%	17.4%
		neg	13.6%	14.3%
		bld	12.0%	12.0%

Table 4.3: Affective pictures classification using one 1.5 sec window

Table 4.3 presents the result of the experiment. As we can see such approach gives poor results. Most accurate result is 29.3%, which is fairly bad.

DFT of first 0.5 seconds ($l = 0.5, \omega = 1$)

It is natural to presume that reaction is most expressed during the first moments of observing the picture. To test that hypothesis we converted the signal to the same instances as before (72 per type), but the window was set to the first 0.5 seconds of the epoch.

Algorithm	Accuracy	Class	Precision	Recall
OneR	23.8%	sex	22.7%	17.9%
		pos	35.8%	20.0%
		ntr	25.8%	34.8%
		neg	17.8%	38.1%
		bld	27.3%	12.0%
J48	20.5%	sex	21.9%	25.0%
		pos	23.1%	12.0%
		ntr	16.1%	21.7%
		neg	22.2%	28.6%
		bld	21.1%	16.0%
Naïve-Bayes	27.9%	sex	28.0%	25.0%
		pos	29.7%	44.0%
		ntr	21.7%	21.7%
		neg	40.0%	28.6%
		bld	22.7%	20.0%
SMO	22.1%	sex	28.0%	25.0%
		pos	19.4%	24.0%
		ntr	10.5%	8.7%
		neg	24.1%	33.3%
		bld	27.8%	20.0%

Table 4.4: Affective pictures classification using one 0.5 sec window

The result changed in the way that now most accurate result is given by the Naïve-Bayes algorithm rather than OneR. F1 score with Naïve-Bayes is 27.5%.

DFT of moving window with length 0.2 seconds and sampling rate 10 Hz ($l = 0.2, \omega = 10$)

In the following experiments we use moving window instead of static one. Moving window means that we take a new window after each τ seconds, so that windows mostly overlap with each other. We compute the DFT of each window and consider it as separate instance. Number of the instances per type is now considerably higher: 1107 instances of **sex** type, 1101 of **pos**, 1103 of **ntr**, 1095 of **neg** and 1105 of **bld**.

Algorithm	Accuracy	Class	Precision	Recall
OneR	19.9%	sex	22.0%	19.9%
		pos	17.8%	17.0%
		ntr	21.6%	20.9%
		neg	17.9%	18.8%
		bld	20.6%	23.1%
J48	22.7%	sex	21.7%	22.5%
		pos	21.3%	21.7%
		ntr	25.1%	23.3%
		neg	23.4%	22.5%
		bld	22.1%	23.4%
Naïve-Bayes	22.5%	sex	25.0%	14.1%
		pos	22.5%	13.5%
		ntr	24.4%	25.9%
		neg	22.5%	46.9%
		bld	16.8%	11.0%
SMO	25.7%	sex	28.8%	29.8%
		pos	24.5%	28.3%
		ntr	27.1%	27.5%
		neg	25.5%	22.5%
		bld	21.9%	20.1%

Table 4.5: Affective pictures classification with 0.2 sec window and 10 samples per second.

Table 4.5 presents result of the first experiment with moving window. Now most accurate result is given by SMO algorithm, and F1 score is 25.6%, which is still unsatisfactory.

DFT of moving window with length 0.5 seconds and sampling rate 10 Hz ($l = 0.5$, $\omega = 10$)

Next we try to increase the size of the window. Distribution of the instances is: 1107 of **sex** type, 1097 of **pos**, 1096 of **ntr**, 1101 of **neg** and 1109 instances of **bld** type.

Algorithm	Accuracy	Class	Precision	Recall
OneR	20.7%	sex	19.4%	17.2%
		pos	21.2%	23.3%
		ntr	19.1%	19.7%
		neg	21.7%	17.8%
		bld	22.0%	25.9%
J48	27.9%	sex	29.5%	31.1%
		pos	29.0%	29.4%
		ntr	27.4%	28.7%
		neg	27.0%	25.7%
		bld	26.4%	24.5%
Naïve-Bayes	26.7%	sex	45.1%	12.1%
		pos	26.7%	12.8%
		ntr	27.0%	43.9%
		neg	24.4%	48.5%
		bld	25.2%	15.8%
SMO	42.2%	sex	42.2%	52.0%
		pos	43.0%	46.8%
		ntr	43.1%	41.2%
		neg	41.3%	36.1%
		bld	41.3%	34.9%

Table 4.6: Affective pictures classification with 0.5 sec window and 10 samples per second.

Table 4.6 shows that the number of instances correctly classified with SMO algorithm has increased significantly – F1 score is 42%. Other algorithms as well show slightly better results. We assume that wider window is more suitable for our type of data.

DFT of moving window with length 0.2 seconds and sampling rate 20 Hz ($l = 0.2, \omega = 20$)

Let us see what happens if we increase the sampling rate, but leave the length of the window the same. Number of instances is: 2304 of **sex** type, 2303 of **pos**, 2301 of **ntr**, 2304 of **neg** and 2272 instances of **bld** type.

Algorithm	Accuracy	Class	Precision	Recall
OneR	20.6%	sex	20.2%	21.8%
		pos	20.2%	20.8%
		ntr	19.4%	18.9%
		neg	23.8%	22.0%
		bld	19.7%	19.7%
J48	24.3%	sex	24.3%	28.5%
		pos	24.5%	24.4%
		ntr	23.4%	22.7%
		neg	25.8%	23.2%
		bld	23.7%	23.0%
Naïve-Bayes	25.4%	sex	28.7%	12.5%
		pos	27.2%	6.4%
		ntr	23.8%	62.2%
		neg	26.1%	26.2%
		bld	28.0%	19.1%
SMO	31.6%	sex	30.7%	35.0%
		pos	26.9%	25.4%
		ntr	33.0%	36.4%
		neg	31.8%	26.9%
		bld	35.6%	34.8%

Table 4.7: Affective pictures classification with 0.2 sec window and 20 samples per second.

If we compare results in tables 4.5 and 4.7 we will see that increasing the size of the windows also helped us to increase the accuracy of our classification. Best F1 score is 31.5% with SMO algorithm. Next logical step is to lengthen the window and increase sampling rate simultaneously.

DFT of moving window with length 0.5 seconds and sampling rate 20 Hz ($l = 0.5, \omega = 20$)

Number of instances here is almost the same in the previous dataset: 2293 of sex type, 2298 of pos, 2288 of ntr, 2297 of neg and 2302 instances of bld type.

Algorithm	Accuracy	Class	Precision	Recall
OneR	20.9%	sex	23.6%	25.7%
		pos	22.8%	23.0%
		ntr	19.3%	20.8%
		neg	18.4%	16.5%
		bld	20.2%	18.8%
J48	38.5%	sex	40.0%	38.6%
		pos	39.0%	40.0%
		ntr	37.4%	38.1%
		neg	36.5%	35.3%
		bld	39.4%	40.4%
Naïve-Bayes	30.0%	sex	28.3%	0.43%
		pos	34.0%	20.3%
		ntr	27.3%	34.1%
		neg	29.6%	29.9%
		bld	35.8%	22.6%
SMO	52.3%	sex	48.9%	51.9%
		pos	53.7%	54.2%
		ntr	51.8%	54.0%
		neg	56.0%	51.8%
		bld	51.7%	49.9%

Table 4.8: Affective pictures classification with 0.5 sec window and 20 samples per second.

As we can see increasing both window length and sampling rate gave most accurate result of 52.4%. Next obvious step is to see how far we can get if we keep increasing those parameters and where is the boundary when increasing will not do any good any more. Further experiments with altering windows length are sampling rate gave no better result than 52.4%.

4.4 Results

In this section we give an overview and charts about the results we achieved. Figure 4.2 shows the results of classifying eye blinks dataset.

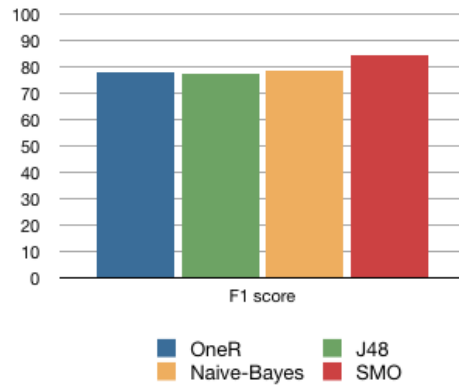


Figure 4.2: Eye blink classification results

Comparison chart of the results of our next experiment are shown on the Figure 4.3. With Naïve-Bayes algorithm we classify *left* and *right* mental

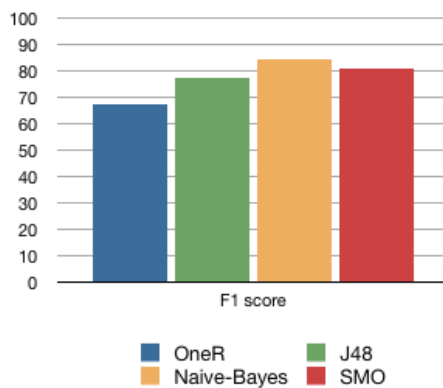


Figure 4.3: Eye blink classification results

states with score of 84%.

As the result of the experiment with the affective pictures dataset we were able to correctly classify half (52.4%) of the pictures. In other words by looking at the subject's brain signal we are able to tell which kind of picture is being shown to the subject at current moment of time with 52.4% accuracy. This result proves that technology works and can be used to monitor human's emotional state, which can be used both in BCI applications and other research involving analyzing work of the human brain. Certainly this result is not the maximal one, in the work by Frantzidis et al. [FBK⁺10]

the result of 77.68% of correctly recognized pictures was achieved. IAPS (International Affective Picture System) [iap] was used as the picture set and C4.5 algorithm for training the classification model.

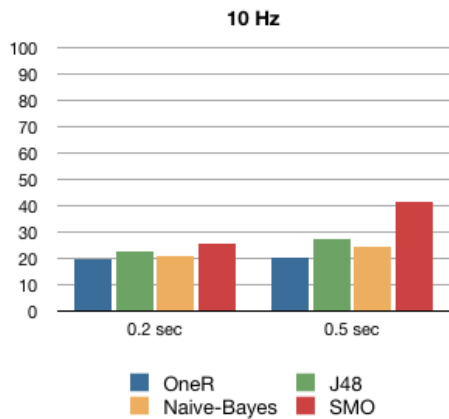


Figure 4.4: F1 scores with moving window and $\omega = 10$

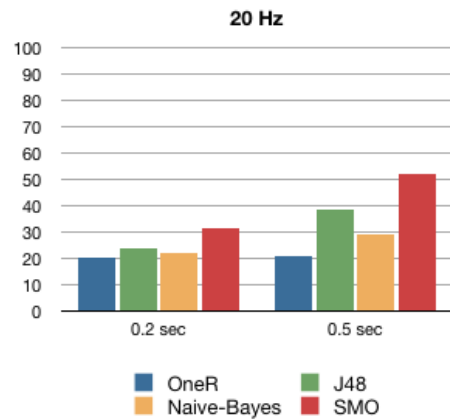


Figure 4.5: F1 scores with moving window and $\omega = 20$

Figures 4.4 and 4.5 show comparison chart for the last 4 experiments. We can see how altering the parameters l and ω affects the results of the classification. SMO algorithm (WEKA's implementation of SVM) shows the best result of 52.4% with $l = 0.5$ seconds and $\omega = 20$.

Summary

We had a look at EEG devices and EEG based BCI technology, which is becoming more and more popular these days. During last few years devices which are designed for wide range of users appeared on the market. According to advertisements, these device could allow human to control the computer with power of thought. But in the real applications, to make technology more functional, these devices read not only brainwaves, but also mimics, pulse and other biometrical parameters. We were interested in how much can we achieve if we use only brainwave signal processing and classification. During the experiments we used data from two different EEG devices. First is inexpensive, aimed for wide range of users Emotiv EPOC with 14 electrodes and second is high-end Biosemi AcitveTwo with 32 electrodes. Two experiments were held and analyzed in this work

1. Distinguishing between *right* and *left* mental states
2. Training a model, which could recognize which kind of 5 kinds of affective pictures subject was shown by reading his brain activity

In the first experiment best result was achieved using Naïve-Bayes algorithm. With 84% accuracy trained model was able to classify brain signal and say if subject was thinking *left* or *right*.

In the second experiment best result of 52.4% accuracy was achieved with SMO algorithm, major accuracy improvements were achieved by enlarging the size of the window and sampling frequency. Best result of 52.4% shows that only by looking at the subject's brain signal, model was able to correctly detect kind of the half of the pictures showed to the subject. This result is interesting and shows that future work in this direction can give even better results.

Experiment with the pictures also shows that EEG technology makes it possible to read human's emotional states. This can be used in BCI applications and other researches, which are related to the human's brain, psychology, for example.

Cheaper devices provide worse signal, but inherit all useful properties. They can be used for simpler tasks, where amount of mental states to recognize is small.

Acknowledgements

We gratefully acknowledge prof. Jüri Allik, Andero Uusberg, PhD, and Kairi Kreegipuu, PhD, from the Department of Psychology at Tartu University for consulting on questions related to EEG technology and providing the affective pictures dataset.

Mustride tuvastamine mitteinvasiivse EEG tehnoloogial baseeruv Aju-Arvuti liideses

Bakalaureusetöö (6 EAP)
Ilja Kuzovkin
Resüme

Töö põhieesmärk on uurida aina populaarsemaks muutuvat EEG tehnoloogial baseeruva Aju-Arvuti liidese võimalusi. Viimaste aastate jooksul on turule jõudnud seadmed, mis on loodud spetsiaalselt tavakasutajate jaoks. Reklaami järgi võimaldavad nad kontrollida arvutit *mõttega*. Kuid tege-
likkuses, selleks, et teha tehnoloogiat töökindlamaks, üritavad need seadmed lugeda ka inimese miimikat, pulssi ja muud sellist. Meid huvitas aga just see, kui palju on võimalik saavutada ainult ajusignaali lugemisega. Eksperimendideks kasutasime andmeid kahest erinevast seadmest. Esimeseks on tavakasutajale orienteeritud Emotiv EPOC 14 elektroodiga ja teiseks tõsisem seade Biosemi ActiveTwo 32 elektroodiga. Töö käigus uurime kahe eksperimendi tulemusi:

1. *parem* ja *vasak* mõtete eristamine.
2. Emotsionaalselt erinevate piltide eristamine.

Esimese eksperimendi käigus parim tulemus oli saavutatud Naïve-Bayes algoritmiga. 84% täpsusega suutis meie mudel klassifitseerida ajusignaale ja teha kindlaks millal inimene mõtleb *paremale* ja millal *vasakule*.

Piltide eristamise eksperimendis parim tulemus on saadud SMO algoritmiga, täpsus kasvas koos akna ja sageduse suurendamisega. Nende parameetrite edaspidine suurendamine ei andnud täpsuse kasvu. Aga juba käesolev tulemus, et 5 pildi puhul algoritm oli suuteline ainult ajusignaali

järgi pooltel (52.4%) juhtumitel selgeks tegema, mis pildiga antud ajamomendil tegu on, on väga huvitav ja näitab, et edasine töö võiks anda isegi paremat tulemust.

Piltidega eksperiment näitab ka, et EEG tehnoloogia abil saab tuvastada inimese emotsionaalset seisundit, mida saab kasutada nii Aju-Arvuti liideses kui ka uuringutes, mis on seotud inimese ajuga, näiteks psühholoogias.

Ka odavamad tavakasutaja jaoks loodud liidesed säilivad need omadused. Neid saaks kasutada lihtsamate ülesannete lahendamiseks, kus eristatavate emotsionaalsete seisundite arv ei ole suur.

Bibliography

- [bioa] Biosemi ActiveTwo prices (<http://www.biosemi.com/faq/prices.htm>).
- [biob] Users of Biosemi devices (<http://www.biosemi.com/users.htm>).
- [con] Comparison of consumer bci devices (http://en.wikipedia.org/wiki/comparison_of_consumer_brain-computer_interface_devices).
- [emo] Emotiv webpage (www.emotiv.com).
- [FBK⁺10] Christos A Frantzidis, Charalampos Bratsas, Manousos A Klados, Evdokimos Konstantinidis, Chrysa D Lithari, Ana B Vivas, Christos L Papadelis, Eleni Kaldoudi, Costas Pappas, and Panagiotis D Bamidis. On the classification of emotional biosignals evoked while viewing affective pictures: an integrated data-mining-based approach for healthcare applications. *IEEE Trans Inf Technol Biomed*, 14(2):309–318, Mar 2010.
- [Fis91] Bruce J. Fisch. *Spehlmann's EEG Primer*. ELSEVIER, 1991.
- [HFL10] Christoph S Herrmann, Ingo Frund, and Daniel Lenz. Human gamma-band activity: a review on cognitive and behavioral correlates and network models. *Neurosci Biobehav Rev*, 34(7):981–992, Jun 2010.
- [iap] International affective picture system (IAPS) (<http://csea.phhp.ufl.edu/media.html>).
- [KABG⁺06] Elif Kirmizi-Alsan, Zubeyir Bayraktaroglu, Hakan Gurvit, Yasemin H Keskin, Murat Emre, and Tamer Demiralp. Comparative analysis of event-related potentials during go/nogo and cpt: decomposition of electrophysiological markers of response inhibition and sustained attention. *Brain Res*, 1104(1):114–128, Aug 2006.
- [KC06] Michael A Kisley and Zoe M Cornwell. Gamma and beta neural activity evoked during a sensory gating paradigm: effects

- of auditory, somatosensory and cross-modal stimulation. *Clin Neurophysiol*, 117(11):2549–2563, Nov 2006.
- [KSO07] Noriaki Kanayama, Atsushi Sato, and Hideki Ohira. Cross-modal effect with rubber hand illusion and gamma-band activity. *Psychophysiology*, 44(3):392–402, May 2007.
- [NYC04] Sander Nieuwenhuis, Nick Yeung, and Jonathan D Cohen. Stimulus modality, perceptual overlap, and the go/no-go n2. *Psychophysiology*, 41(1):157–160, Jan 2004.
- [PP07] Satu Palva and J. Matias Palva. New vistas for alpha-frequency band oscillations. *Trends Neurosci*, 30(4):150–158, Apr 2007.
- [PR04] E. Frank P. Reutemann, B. Pfahringer. 17th australian joint conference on artificial intelligence (ai2004). In *Proper: A Toolbox for Learning from Relational Data with Propositional and Multi-Instance Learners.*, 2004.
- [WF05] Ian H. Witten and Eibe Frank. *Data Mining: Practical Machine Learning Tools and Techniques*. ELSEVIER, 2005.
- [wika] Brain-computer interface (http://en.wikipedia.org/wiki/brain-computer_interface).
- [wikb] Nerve cell (http://en.wikipedia.org/wiki/nerve_cell).
- [wikc] Support vector machine (http://en.wikipedia.org/wiki/support_vector_machine).
- [Won10] Cheuk-Wah Wong. The brain, thinking, and memory: A theory based on pathophysiology of amnesia. *Neurology*, 100, March 2010.
- [waud] Physiological and histological investigation of structure and function of the normal auditory system (<http://www.ihr.mrc.ac.uk/index.php/research/current/1>).
- [YR10] G. Gibert M. Congedo E. Maby V. Delannoy O. Bertrand A. Lecuyer Y. Renard, F. Lotte. Openvibe: An open-source software platform to design, test and use brain-computer interfaces in real and virtual environments. *Presence : teleoperators and virtual environments*, 19, no 1, 2010.